DOI: 10.2352/ISSN.2470-1173.2016.14.IPMVA-380

Toward a Fusion of Optical Coherence Tomography and Hyperspectral Imaging for Poultry Meat Quality Assessment

Seung-Chul Yoon, Brian C. Bowker and Hong Zhuang
U.S. Department of Agriculture - Agricultural Research Service, U.S. National Poultry Research Center, Athens, GA, U.S.A.

Abstract

An emerging poultry meat quality concern is associated with chicken breast fillets having an uncharacteristically hard or rigid feel (called the wooden breast condition). The cause of the wooden breast condition is still largely unknown, and there is no single objective evaluation method or system known for rapidly and non-invasively detecting this quality defect in boneless-skinless chicken breast fillets. Thus, there is an immediate need to develop a rapid and non-invasive sensing technique to detect the wooden breast condition. In this study, sub-surface microstructure and optical properties of poultry meat were measured by optical coherence tomography (OCT) at 930 nm and hyperspectral imaging from 400 to 1,000 nm. The analysis of the measured OCT B scan images showed that the thickness and pattern of the epimysium (the fibrous connective tissue surrounding the muscle tissue) of the meat could be a good feature to differentiate between normal and wooden breast fillets. The OCT signals under the fats and whitish strong connective tissue were smeared with speckle noise so that the epimysium layer edge disappeared under these locations. Because OCT imaging had a small field of view (~1 cm x 1 cm), it was implied that the scanning time of a large area such as a chicken fillet would be very long. On the other hand, hyperspectral imaging was effective to rapidly scan the entire surface of each fillet and detect excessive fats and strong connective tissue although a spectral analysis showed that there was no pronounced difference between mean spectra of normal and wooden breast fillets. The study results suggested that hyperspectral imaging would increase the throughput of OCT imaging while OCT would detect the wooden breast condition, when both modalities were fused. Thus, a fusion of OCT and hyperspectral imaging will provide a sensing tool to rapidly and accurately detect and sort chicken breast fillets with the wooden breast condition.

Introduction

In the U.S. poultry industry, advancements in genetic selection and nutrition of birds have produced large, fast-growing broilers [1, 2]. However, poultry-meat quality defects are also becoming more prevalent in modern large, fast growing broiler chickens [3]. These quality defects are mainly associated with muscle myopathies such as white-striping (white striations parallel to the muscle fibers on the surface of the breast muscle) [4] and the wooden breast condition (breast fillets with an uncharacteristically hard or rigid feel) [5]. The cause of these muscle myopathies (i.e. white striping and wooden breast) is largely unknown. The symptoms of these quality defects include abnormal microstructure and appearance such as severe muscle degeneration and fibrosis (connective tissue irregularity) in the wooden breast condition (WBC) and abnormal accumulation of connective tissue causing excessive white striations on the skin surface in the white striping problem. Currently, there is no single objective evaluation method or system known for rapidly and non-invasively detecting and sorting boneless-skinless breast fillets with these myopathies. Thus, there is an immediate need to develop a rapid and non-invasive sensing and sorting technique to detect these quality defects while measuring the overall quality of fillets.

The purpose of this study was to investigate the potential of optical coherence tomography (OCT) and hyperspectral imaging to measure subsurface microstructure and optical properties (diffusive reflectance/absorption) of wooden breast (WB) fillets. OCT is an interferometric technique capable of non-invasive 1D, 2D, and 3D imaging of subsurface microstructure [6] whereas hyperspectral imaging is an imaging modality to measure optical properties of samples, such as reflectance [7]. The specific objective of the study was to investigate the pros and cons of OCT and hyperspectral for rapid and non-invasive measurement of the wooden breast condition of poultry meat and explore how to fuse these two imaging modalities in practice.

Materials and Methods

Chicken Fillet Samples

As a preliminary study, 14 skinless, boneless breast (pectoralis major) fillets were collected from the deboning line (~3 h postmortem) of a commercial processing plant that slaughters large broilers (7-9 lbs. live weight). The broiler birds were about 8 weeks old. Fillets were selected in collaboration with experienced industry personnel based on the severity of the wooden breast condition (7 normal and 7 severe). Fillets were placed in plastic bags, packed on ice, and transported back to the U.S. National Poultry Research Center in Athens, GA (~40 min). Prevalence of visual defects (white striations, blood splash, excessive viscous fluid on surface, etc.) was recorded. Fillets were trimmed of excess fat and connective tissue and weighed. Note that some fats and connective tissue remained even after the trimming. Grouped into two classes (normal vs. severe) based on the rigidity of the fillet and the palpable severity of the diffuse hardened areas. Figure 1 shows two fillet examples with normal vs. severe wooden breast condition.

Figure 1*. Normal breast fillet (left) and wooden breast fillet (right)*

DOI: 10.2352/ISSN.2470-1173.2016.14.IPMVA-380

OCT Imaging System

OCT is a non-invasive, sub-surface optical imaging modality, providing micrometer resolution and millimeter imaging depth. OCT is based on a theory of low coherence interferometry, where interference of broadband light with low temporal coherence occurs over a distance of micrometers (i.e. a short coherence length). A broadband light source (e.g. a superluminescent diode) in near-infrared wavelength regions (e.g. at around 900 nm and 1,300 nm) is typically used for OCT. The use of a near-infrared light source for OCT allows a better light penetration into biological tissue than the visible light. The basic scanning mechanism of OCT is to form an interferogram by combining the reflected light profiles from the reference arm and at a point in the sample, which is called a single-point A-scan. A B-scan generates a 2D cross-sectional image (called a longitudinal image) in the X (lateral)-Z (depth) plane. A 3D volumetric OCT image can be achieved by multiple line scans (B scans) in an area. A C-scan image, called en face image or transverse image in the X-Y plane can be obtained from a 3D data set.

In this study, a spectral-domain OCT (SD-OCT) imaging system (Callisto, Thorlabs, Newton, NJ, USA) was used to acquire 2D cross-sectional B-scan images. The SD-OCT system consisted of a 930-nm superluminescent diode light source with a 100-nm spectral bandwidth, a scanning system, an objective lens with a 36-mm focal length, a linear CCD array-based spectrometer with 1024 pixels, and an en face video camera with white light and 640 x 480 pixel resolution. The maximum B-scan frame rate for 512 A scans was 2 frames per second. The maximum field of view (FOV) for a 3D scan was 10 mm (X) x 10 mm (Y) x 1.7 mm (Z, depth). In practice, the small FOV and slow frame rate limited the number of B scans and the size of scanning area. In this study, the skin-side surface locations at three major portions (cranial, middle, and caudal) of each fillet were manually selected to measure OCT B-scan images. A total of 41 OCT B-scan images were collected from three locations per each fillet. The length of a B-scan was 8.08 mm and the depth was 1.69 mm. The acquisition time of one B-scan image with 1,040 (X) and 512 (Z) pixels was 2.64 seconds. The pixel resolution was 7.77 μm (lateral) and 3.31 μm (axial), respectively.

Hyperspectral Imaging System

Hyperspectral imaging combines spectroscopy and optical imaging to acquire spatially co-registered images in a pre-defined wavelength range of the electromagnetic spectrum (typically, 400-1,000 or 1,000-2500 nm) to obtain spectral information at each image pixel location in the scanned area. Hyperspectral imaging has shown great potential in safety and quality assessment of food and agricultural products by measuring biological, chemical and physical properties of the products [7, 8]. In fresh red meat, near-infrared spectroscopy has been used to assess tenderness, water-holding capacity, color, pH, marbling, and sensory attributes [9]. Although a hyperspectral imaging system has been successfully developed for the detection of fecal materials [10, 11] and systemic disease [12] in poultry carcasses in a commercial setting, its use for poultry meat quality assessment has been underexplored. It can be hypothesized that detection of the wooden breast condition may be possible through the use of hyperspectral imaging. Being able to accurately detect the wooden breast condition using hyperspectral imaging online would allow processors to produce more uniform products in terms of meat quality through product segregation and to more accurately monitor how broiler production, handling, and slaughtering practices influence the occurrence of the wooden breast condition.

The hyperspectral imaging system used for this study was a pushbroom line scanner in the visible and near-infrared (VNIR) spectral wavelength range from 400 to 1,000 nm. This hyperspectral imaging system consisted of a hyperspectral camera, a copy stand to which the camera was attached, and a computer that controlled the hyperspectral image acquisition. Illumination was provided by two soft boxes with tungsten lamps. The hyperspectral camera (Themis Vision Systems, Richmond, VA, USA) consisted of a VNIR spectrograph (ImSpector V10M, Specim, Oulu, Finland), a 16-bit 5.5 megapixel sCMOS detector (pco.edge, PCO-Tech Inc., Romulus, MI, USA), a focal plane scanner, and a front lens (Zeiss Distagon T* 35mm f/2 ZE, Zeiss, Thornwood, NY, USA). The front lens unit was moved by a motion control in order to scan the field of view line by line. The spectrograph had a nominal spectral range between 350 nm and 1000 nm. The sCMOS camera provided a 2560 x 2160 pixel resolution. The hyperspectral imaging system captured a series of 2D spectral images of the target with each image possessing spatial information along the x-axis and spectral information along the y-axis. These 2D spectral images were combined to create a 3D hyperspectral image data cube via HyperVisual software (Themis Vision Systems, Richmond, VA, USA) on the fly. Diffuse reflectance was measured. The measured digital numbers at each pixel in the hyperspectral image were normalized (i.e. calibrated) to relative reflectance R using a 99% reflectance Spectralon® target (25.4 cm × 25.4 cm, SRT-99-100, Labsphere, North Sutton, NH, USA). The dimensions of one hyperspectral image data cube were 1,351 (width) x 751 (lines) x 836 (wavelengths, 400-1,000 nm). The noise in the measured spectra was reduced by a Savitzky-Golay smoothing filter (window size: 25; order of moment: 4) at each pixel position. After that, the calibrated hyperspectral images with relative reflectance values were stitched together into a single image mosaic, as shown in Figure 2 for normal and severe WB fillets, respectively.

Data Processing and Analysis

In SD-OCT, the signal processing algorithm to obtain the A scan profile from an interferogram is based on fast Fourier transform (FFT). The basic steps to create the depth-resolved intensity profile of a single A scan were the acquisition of a spectrogram (i.e. a spectrum), background subtraction, re-sampling, and inverse FFT [6, 13]. The hyperspectral images were analyzed by first creating regions-of-interest (ROIs) using ENVI software (Exelis Visual Information Solutions, Boulder, CO, USA). The ROIs were obtained to extract spectral information in user-defined regions and to train/test classification and prediction models. Two types of ROIs were prepared. One type was to define the ROIs where the OCT images were collected. The other type of the ROIs was to define the representative spectra of meat, excessive fats, and whitish connective tissue. Notice that the excessive fats and connective tissue including white stripes still remained after sample trimming.

The microstructure of chicken breast fillets was analyzed from the OCT B scan images. The structural difference between normal and severe wooden breast fillets was analyzed qualitatively and quantitatively. In this study, the analysis of the images was limited to the first layer of meat (muscle). A histology study with tissue samples spatially associated with OCT images is highly recommended in the future in order to better explain the OCT images and the structure information that OCT reveals. The area of

DOI: 10.2352/ISSN.2470-1173.2016.14.IPMVA-380

the first layer was objectively analyzed by image processing including histogram equalization, noise filtering, morphological filtering, and intensity thresholding. A classification model that was used to classify meat, fat and connective tissue was based on principal component analysis (PCA) and linear discriminant analysis (LDA) using principal component (PC) scores on the PC domain. Notice that the OCT images and hyperspectral images were not spatially co-registered because the primary goal of this study was to quickly investigate the potential of both OCT and hyperspectral imaging and evaluate the pros and cons of each imaging modality.

Results and Discussion

Figure 2 shows the mosaics of color video frames overlaid with the OCT B-scan lines and the mosaics of color-composite images obtained from hyperspectral images overlaid with the regions of interest where the OCT probe was pointed. Each OCT scan line (a red horizontal arrow on each video frame) was set within about 8 mm x 10 mm area. The color video frames of normal and WB fillets were arranged in 3 rows (probing locations at cranial, middle, and caudal parts from top to bottom) and 7 columns (fillet samples) in each mosaic, respectively.

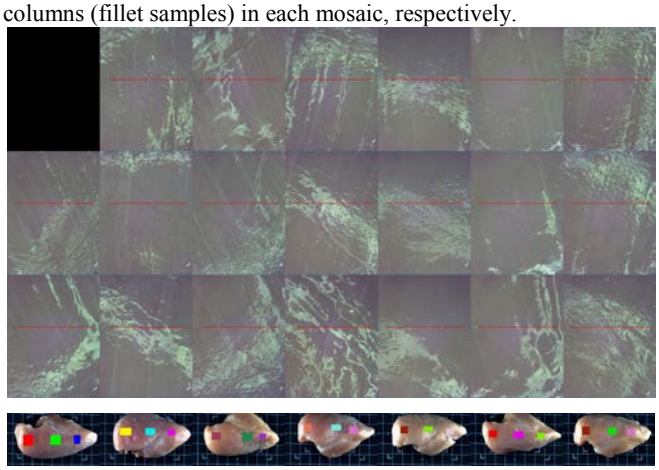

(a) Normal fillets

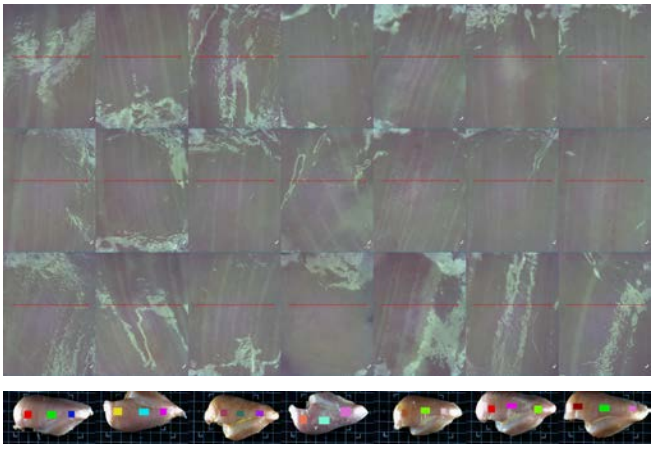

(b) Wooden breast fillets

Figure 2. *Mosaics of color video frames overlaid with the OCT scan lines (red arrows) and mosaics of color-composite images of whole fillets overlaid with the regions of interest (boxes) where the OCT probe was pointed.*

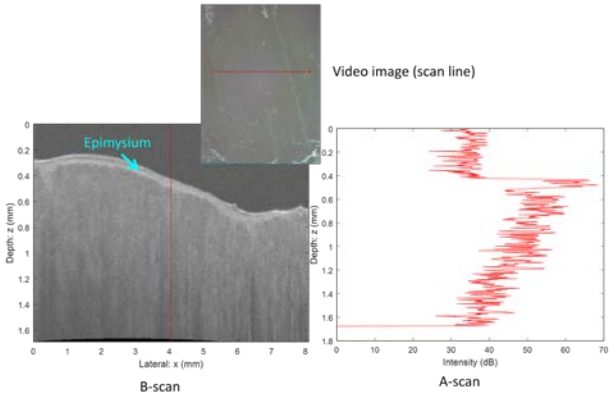

(a) Normal

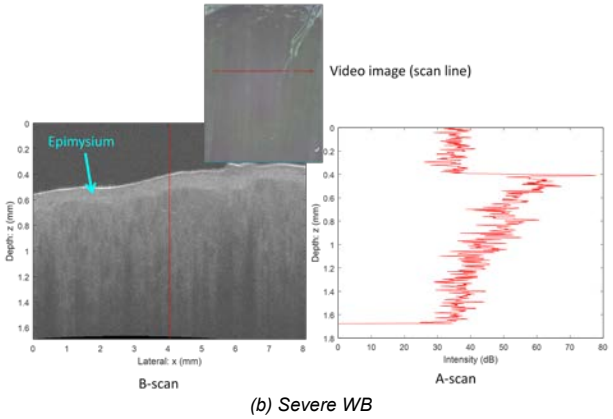

(b) Severe WB

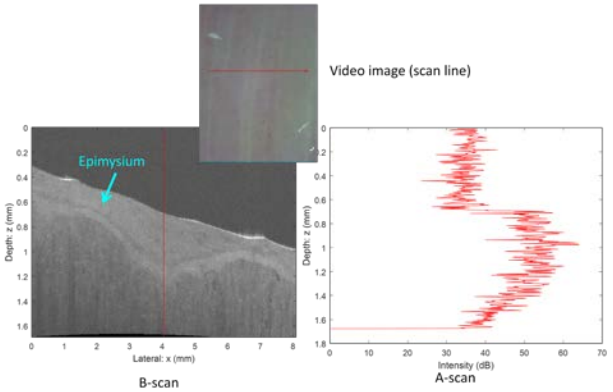

(c) Severe WB with strong white stripes

Figure 3. *Example video frames, scan lines, B scans, and A scans for (a) normal fillet, (b) severe WB fillet and (c) severe WB fillet with strong white stripes.*

Similarly, the hyperspectral images were mosaicked in 7 columns (fillet samples) from left to right in Figure 2. The visual difference between normal and severe WB fillet images was minor, strongly implying that color vision would not be appropriate to detect the WBC. Because the degree of white stripes appeared to be highly related to the severity of WBC of each fillet, the ability of white stripes to measure the severity of WBC needs to be investigated in the future.

The analysis of the cross-sectional OCT images suggested that the first layer of poultry muscle tissue might have different optical properties (e.g. refractive index and reflectivity). The first layer is called epimysium. The epimysium is a specialized form of the deep fascia that surrounds the muscle and is continuous with

DOI: 10.2352/ISSN.2470-1173.2016.14.IPMVA-380

the fascia. The epimysium is fibrous connective tissue that is comprised mostly of densely packed and interconnected collagen molecules. Figure 3 shows three examples of video frames, OCT scan lines, B scans, and A scans for one normal fillet and two severe WB fillets. Figure 4 shows the mosaics of OCT B-scan images for normal (top) and WB fillets (bottom). When there was neither strong connective tissue nor white striping visible on the fillet surface as in Figure 3(a) and 3(b), the corresponding epimysium was clearly visible and pronounced with contrasting edges along the scan line. However, when either strong connective tissue or white striping was present in the scanning path, the OCT signals under the fats and whitish strong connective tissue were smeared with speckle noise so that the epimysium layer edge disappeared. For example as in row 3 and column 4 of WB fillet mosaic in Figure 4, when the OCT probe scanned the fatty area, the epimysium was no longer clearly visible and only speckle noise was observed under the surface. The air-epimysium interface was more pronounced in normal fillets. These observations implied that the excessive fats and connective tissue including strong white stripes would make the detection of WBC more complex and difficult because normal fillets may also have excessive fats and strong connective tissue on their surfaces.

The thickness and the area of the epimysium were measured by image processing. The processing results are shown as binary images in Figure 5. The estimated thickness of the epimysium was about 0.097 mm and 0.214 mm for normal and severe WBC fillets, respectively. The area of the epimysium was 15.71 mm^2 And 36.29 mm^2 for normal and severe WBC fillets, respectively.

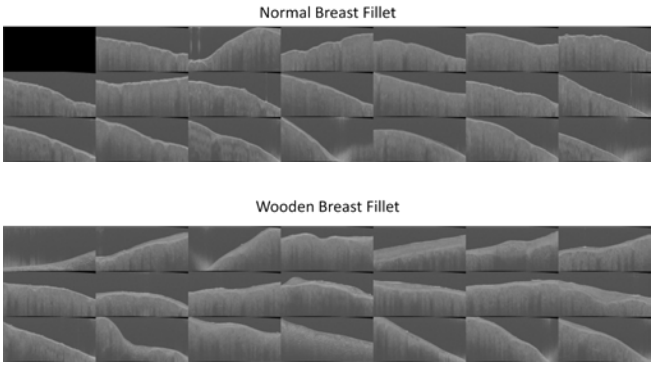

***Figure 4**. Mosaics of OCT B-scan images: Normal (top) and WB fillets (bottom).*

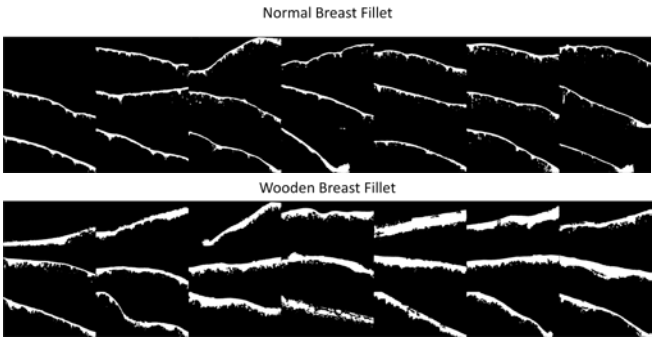

***Figure 5**. Mosaics of processed B-scan images showing the potentially epimysium layers: Normal (top) and WB (bottom) fillets.*

The mean spectra obtained from the hyperspectral images are shown in Figure 6. The overall shape and reflectance of the mean spectra of normal and WB fillets were very similar across the entire spectral range from 400 to 1,000 nm. This observation suggested that there were no obvious spectral features to use for detecting WBC. However, a more close examination revealed that although the differences are subtle, the spectral regions between 400 nm and 425 nm and between 525 nm and 600 nm could be potential spectral areas for a further investigation in the future. Figure 7 shows the mean spectra of fat, meat (muscle tissue) and whitish connective tissue. The mean spectral analysis clearly indicated that hyperspectral imaging could differentiate these three materials on the surface of each chicken fillet. The PCA-LDA classification results for fat, meat and connective tissue, as shown in Figure 8, implied that the hyperspectral imaging would be appropriate to detect these normal features of chicken fillets

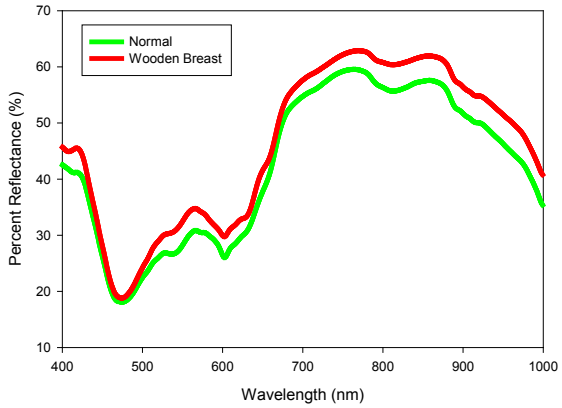

***Figure 6**. Mean spectra of normal and WB fillets.*

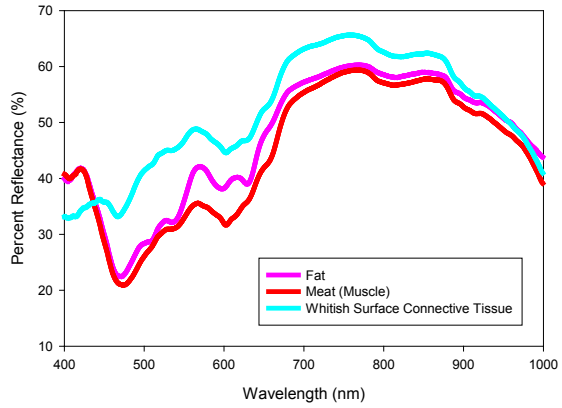

***Figure 7**. Mean spectra of fat, meat (muscle) and whitish surface connective tissue.*

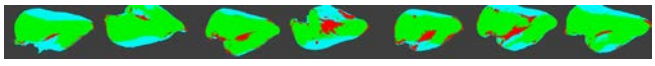

***Figure 8**. Classification of fat, meat and connective tissue on severe WB fillets.*

Conclusion

Spectral domain OCT and hyperspectral imaging modalities were examined to investigate the potential of both techniques for rapid and non-invasive detection and sorting of boneless, skinless poultry breast fillets with the wooden breast condition. The OCT imaging showed a potential for differentiating between

DOI: 10.2352/ISSN.2470-1173.2016.14.IPMVA-380

microstructures of normal and wooden breast fillets. The analysis of the OCT cross-sectional images showed that the epimysium (outer later) encompassing chicken breast muscle tissue with the wooden breast condition was consistently thicker than normal fillets. The epimysium thickness of the wooden breast filets was about 2 times larger than normal fillets. Hyperspectral imaging showed that it could distinguish between fat, muscle tissue and excess connective tissue and assess their quantities. Although the capability to detect the wooden breast condition using hyperspectral imaging was limited, hyperspectral imaging combined with OCT imaging would increase the throughput of OCT imaging. Thus, a fusion of OCT and hyperspectral imaging is recommended to rapidly and accurately detect and sort chicken breast fillets with the wooden breast condition.

References

[1] G. B. Havenstein, P. R. Ferket, and M. A. Qureshi, "Carcass composition and yield of 1957 vs. 2001 broilers when fed representative 1957 and 2001 broiler diets," *Poultry Science*, vol. 82, pp. 1509-1518, 2003.

[2] G. B. Havenstein, "Performance changes in poultry and livestock following 50 years of genetic selection," *Lohmann Information*, vol. 41, pp. 30-37, 2006.

[3] M. Petracci and C. Cavani, "Muscle growth and poultry meat quality issues," *Nutrients*, vol. 4, pp. 1-12, 2012.

[4] V. A. Kuttappan, Y. Lee, G. F. Erf, J. F. Meullenet, and C. M. Owens, "Consumer acceptance of visual appearance of broiler breast meat with varying degrees of white striping," *Poultry Science*, vol. 91, pp. 1240-1247, 2012.

[5] H. K. Sihvo, K. Immonen, and E. Puolanne, "Myodegeneration with fibrosis and regeneration in the pectoralis major muscle of broilers," *Veterinary. Pathology,* vol. 51, 619-623, 2014.

[6] J. A. Izatt and M. A. Choma, "Theory of optical coherence tomography," *Optical Coherence Tomography Technology and Applications,* Springer, pp. 47-72, 2008.

[7] A. A. Gowen, C. P. O'Donnell, P. J. Cullen, G. Downey, and J. M. Frias, "Hyperspectral imaging–an emerging process analytical tool for food quality and safety control," *Trends in Food Science and Technology*, vol. 18, 590-598, 2007.

[8] D. W. Sun, *Hyperspectral Imaging for Food Quality Analysis and Control*, Academic Press, 2010.

[9] D. Alomar, C. Gallo, M. Castaneda, and R. Fuchslocher, "Chemical and discriminant analysis of bovine meat by near infrared reflectance spectroscopy (NIRS)," *Meat Science*, vol. 63, 441-450, 2003.

[10] B. Park, K. C. Lawrence, W. R. Windham, and R. J. Buhr, "Hyperspectral imaging for detecting fecal and ingesta contaminants on poultry carcasses," *Trans. ASAE*, vol. 45, 2017-2026, 2002.

[11] S. C. Yoon, B. Park, K. C. Lawrence, W. R. Windham, and G. W. Heitschmidt, "Line-scan hyperspectral imaging system for real-time inspection of poultry carcasses with fecal material and ingesta," *Computers and Electronics in Agriculture*, vol. 79, 159-168, 2011.

[12] K. Chao, C. C. Yang, Y. R. Chen, M. S. Kim, and D. E. Chan, "Hyperspectral-multispectral line-scan imaging system for automated poultry carcass inspection applications for food safety," *Poultry Science*, vol. 86, 2450-2460, 2007.

[13] M. Ali and R. Parlapalli, "Signal processing overview of optical coherence tomography systems for medical imaging," *Texas Instrument White Paper*, SPRABB9, 2010.

Author Biography

Seung-Chul Yoon *received his Ph.D. in electrical engineering from University of Illinois at Urbana-Champaign (2003). He worked at HRL Laboratories (1999), Science Applications International Corporation (2001-2003), and DVT Corporation (2004). Since 2004, he has worked as a research electronics engineer in the Quality and Safety Assessment Research Unit at the USDA-ARS in Athens, GA, USA. Dr. Yoon has over 20 years of experience in developing machine vision and image processing algorithms and 10+ years in hyperspectral imaging. Dr. Yoon's research area is development of rapid optical imaging technology to solve food safety and quality problems faced in the food industry.*

Brian C. Bowker *received his Ph.D. in Meat Science and Muscle Biology from Purdue University (2003).He was a U.S. congressional science fellow during 2003 and 2004. From 2004 to 2011, he worked in the Food Technology & Safety Laboratory at the USDA-ARS in Beltsville, MD, USA. Since 2011, he has worked as a research chemist in the Quality and Safety Assessment Research Unit at the USDA-ARS in Athens, GA, USA. Dr. Bowker has extensive research experience on meat quality attributes in both red meat and poultry. Recent research projects have focused on muscle protein alterations and the mechanisms controlling poultry meat quality as well as the development of rapid, non-invasive technologies for measuring poultry meat quality.*

Hong Zhuang *received his Ph.D. in Nutritional Science from University of Kentucky (1996) He worked at EPL Technologies (1998-2003), Redi-cut Foods (2003-2006), and Chiquita Brands International (2003-2006). Since 2006, he has worked as a research food technologist in the Quality and Safety Assessment Research Unit at the USDA-ARS in Athens, GA, USA. Dr. Hong Zhuang has more than 20 years of research experience and training in the field of instrumental analyses of sensory-related compositions and properties of food products, sensory evaluation techniques for food quality assessment, spectroscopic analysis and statistical modeling between sensory quality attributes and instrumental parameters.*